

# Measuring phonon dephasing with ultrafast pulses using Raman spectral interference

F. C. Waldermann, Benjamin J. Sussman,<sup>\*</sup> J. Nunn, V. O. Lorenz, K. C. Lee, K. Surmacz, K. H. Lee, D. Jaksch, and I. A. Walmsley

Clarendon Laboratory, University of Oxford, Parks Road, Oxford OX1 3PU, United Kingdom

P. Spizziri, P. Olivero, and S. Prawer

Center for Quantum Computer Technology, School of Physics, The University of Melbourne, Parkville, Victoria 3010, Australia

(Received 12 April 2008; revised manuscript received 1 September 2008; published 9 October 2008)

A technique to measure the decoherence time of optical phonons in a solid is presented. Phonons are excited with a pair of time-delayed 80 fs near infrared pulses via spontaneous transient Raman scattering. The spectral fringe visibility of the resulting Raman pulse pair, as a function of time delay, is used to measure the phonon dephasing time. The method avoids the need to use either narrow band or few femtosecond pulses and is useful for low phonon excitations. The dephasing time of phonons created in bulk diamond is measured to be  $\tau = 6.8$  ps ( $\Delta\nu = 1.56$  cm<sup>-1</sup>).

DOI: [10.1103/PhysRevB.78.155201](https://doi.org/10.1103/PhysRevB.78.155201)

PACS number(s): 78.30.Am, 81.70.Fy, 65.40.-b, 63.20.Ry

## I. INTRODUCTION

Phonons are a fundamental excitation of solids that are responsible for numerous electric, thermal, and acoustic properties of matter. The lifetime of optical phonons plays an important role in determining these physical properties and has been the subject of extensive study. A technique to measure phonon dephasing times is presented here that utilizes spectral interference of ultrafast infrared laser pulses. Transient coherent ultrafast phonon spectroscopy (TCUPS) offers a number of conveniences for measuring phonon dephasing. TCUPS utilizes commercially available ultrafast pulses (80 fs) and hence does not require a narrow band or extremely short lasers to achieve high spectral or temporal resolution. As well, TCUPS is suitable for measurements in the single phonon excitation regime. The large sampling area and long sampling distance increase the generated Stokes power and avoid sample heating, which is a concern for low-temperature studies. Diamonds are well known for their extraordinary physical properties<sup>1</sup> and also offer interesting prospects for use in quantum information applications.<sup>2-5</sup> As such, diamond has been selected here as the material for demonstration of TCUPS.

Two methods have previously been utilized to measure phonon lifetimes: high-resolution Raman spectroscopy and differential reflectivity measurements. The first is the traditional technique, where the optical phonon lifetime is obtained from high-resolution linewidth measurements of the first-order Raman peak, usually conducted using narrow-band excitation lasers and high-resolution spectrometers.<sup>6</sup> The alternative technique, working in the time domain, can directly show the temporal evolution of the surface vibrations of solids.<sup>7</sup> A femtosecond pump pulse is used to excite a phonon population. The reflectivity (or transmittivity) of a subsequent probe pulse displays a time dependence that follows the vibrational frequency and population of excited phonons. This method was used to study the phonon decay in various solids,<sup>8</sup> their symmetry modes,<sup>9</sup> and their interaction with charge carriers<sup>10</sup> and with other phonons.<sup>11</sup> In these experiments, impulsive stimulated Raman scattering has been established as the coherent phonon generation mechanism.<sup>12,13</sup>

The time-domain experiments utilize the impulsive regime, i.e., laser-pulse lengths much shorter than the phonon oscillation period (inverse phonon frequency). This requirement can be challenging for the application of the differential reflectivity technique to materials with high phonon energies as laser systems with very short pulse lengths are required (e.g., for diamond, sub-10 fs pulses are required to resolve a phonon frequency of 40 THz). On the other hand, TCUPS operates in the transient spontaneous Raman-scattering regime,<sup>14</sup> i.e., pulse lengths much longer than the phonon oscillation period (about 25 fs for diamond), but still much shorter than the phonon decoherence time.<sup>15</sup> Stimulated Raman scattering, which implies large phonon excitations, is often employed in dephasing measurements in order to achieve good signal-to-noise ratios. High phonon population numbers, often referred to as *hot phonons*, can be subjected to an increased decay rate, as previously observed<sup>16</sup> for GaN. By contrast, TCUPS investigates the properties of a phonon excitation by direct analysis of the Stokes spectra generated in the Raman process. The use of single-photon detectors extends the sensitivity of the experiment to low phonon populations including the single phonon level.

## II. EXPERIMENT

The diamond was classified as a type-Ib high-pressure high-temperature (HPHT) sample with a nitrogen impurity concentration of less than 100 ppm. The Stokes shift of diamond<sup>17</sup> is 1332 cm<sup>-1</sup> and the Raman gain coefficient for

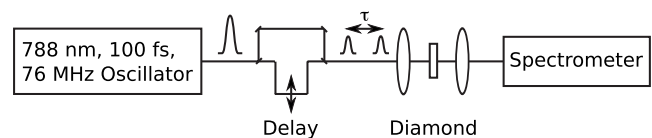


FIG. 1. Experimental setup. An oscillator pulse is split into two time-delayed pulses and focused through the diamond sample. Not shown, a bandpass filter cleans the oscillator pulse before the diamond and a long-pass filter rejects the pump and transmits the Stokes before the spectrometer.

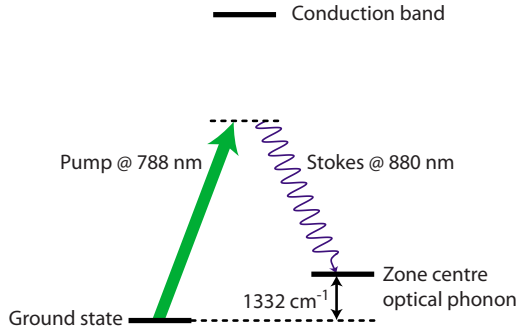


FIG. 2. (Color online) Diamond energy-level schematic. Ground state phonons are excited with the incident 788 nm pump, via a Raman transition, to the optical phonon mode, emitting an 880 nm Stokes pulse.

diamond has been reported<sup>18</sup> as  $g_R = 7.4 \times 10^{-3}$  cm/MW (corrected for  $\lambda = 800$  nm). With pump pulse energies ranging over 1.1...380 pJ, the collinear Stokes emission is calculated as 0.004–1.3 photons per pulse, in agreement with the count rates achieved experimentally. The pump laser had a diameter of  $d \approx 5$  mm and was focused with a  $f = 5$  cm lens resulting in fluences ranging roughly from 0.01 to 5 J/m<sup>2</sup>. The Raman scatter is thus in the spontaneous regime, as verified by a linear pump power dependence ranging over 3 orders of magnitude (see inset of Fig. 5). Therefore, the experiment is performed at powers far below the hot phonon regime.

The experimental setup is depicted in Fig. 1. Phonons are excited, via a Raman transition, with a pair of time-delayed 80 fs, 788 nm pulses (Fig. 2) from a commercial Ti:sapphire oscillator (Coherent Mira). The pulses are focused into a  $2 \times 2 \times 1$  mm diamond with faces polished along [100] plane (Sumitomo). Stokes emission is detected collinearly. The pump laser is spectrally filtered using a bandpass filter to avoid extraneous light at the Stokes frequency, which might seed stimulated emission and which decreases the signal-to-noise ratio when detecting single Stokes photons. The Stokes scatter is detected and spectrally analyzed by means of a 30 cm spectrometer (Andor Shamrock 303i) and an electron multiplying charge coupled device (EM-CCD) (iXon DV887DCS-BV), which is capable of statistical single-photon counting. The gratings were ruled at 150 lines/mm for data in Figs. 3 and 1800 lines/mm for Figs. 4 and 5.

The spectral interference from the pump pair and Stokes pair is shown in Fig. 3. The fringe spacing  $\Delta\lambda$  is as expected

for two time-delayed coherent pulses  $\Delta\lambda = \lambda^2 / c\tau$  [see also Eq. (4) below]. For the excitation pair,  $\lambda$  is the center wavelength of the pump [Fig. 3(b)] and for the generated output Raman pair,  $\lambda$  is the center wavelength of the Stokes [Fig. 3(d)]. The fringe spacing of the Raman output corresponds to the Stokes peak wavelength, confirming that the process is a measure of the coherence of the Raman process. Figure 4(a) shows the fringe visibility reduction as a function of time delay. The fringe visibility  $V = \exp(-\Gamma|\tau|)$  is plotted in Fig. 4(b). The decay time  $\Gamma$  is discussed below. The visibility has been renormalized using the laser visibility for each delay to account for beam walk-off and the spectrometer resolution which artificially reduces visibility due to a sampling effect from the finite pixel size of the spectrometer CCD.

III. THEORY

The observed spectral interference visibility can be considered from two perspectives. In the first, the visibility decay arises due to fluctuations of the phase in the classical fields. Each input laser pulse excites optical phonons, via a Raman transition (Fig. 2), which in turn causes the emission of two Stokes pulses. That is, the Raman interaction maps the electric field of the two input pulses to two output Stokes shifted pulses

$$E_{\text{Stokes}} = E_1(t) + E_2(t). \tag{1}$$

The phase of the first Stokes pulse  $E_1$  is determined spontaneously, but the phase (and amplitude at stimulated intensities) of the second pulse  $E_2$  is influenced by the coherence maintained by the phonon in the system following the first pulse, so that the output field may also be rewritten as

$$E_{\text{Stokes}}(t) = E_1(t) + e^{i\theta} E_1(t - \tau), \tag{2}$$

where  $\tau$  is the time delay between the input pulses and  $\theta$  is the spontaneously fluctuating phase difference between the pulses. The spectral intensity of the Stokes pulse pair

$$|E_{\text{Stokes}}(\omega)|^2 = 2|E_1(\omega)|^2 [1 + \cos(\omega\tau + \theta)] \tag{3}$$

contains interference fringes whose position depends on the relative phase  $\theta$ . Shot-to-shot, decoherence causes spontaneous fluctuations in  $\theta$  and the fringe pattern loses visibility. At longer delays  $\tau$ , the fluctuations increase, eventually reducing the visibility of any integrated fringe pattern to zero. Assuming a Lorentzian line shape with width  $\Gamma$  for the distribution of the phase  $\theta$ , the shot-to-shot averaged spectral intensity is broadened to

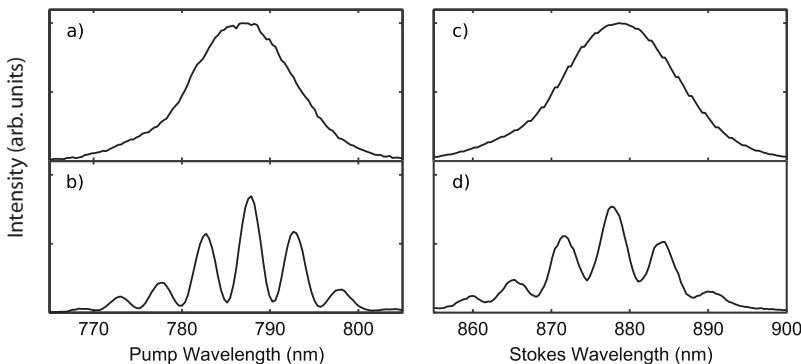


FIG. 3. Example spectral interference for a delay  $\tau = 0.39$  ps. Spectra of the broadband excitation laser (left) and the Stokes signal of diamond (right). The single pulse data in (a) and (c) show the pump-laser spectrum and the corresponding broadband Raman spectrum, respectively. Spectral interference fringes appear for coherent pulse pairs in (b) and (d).

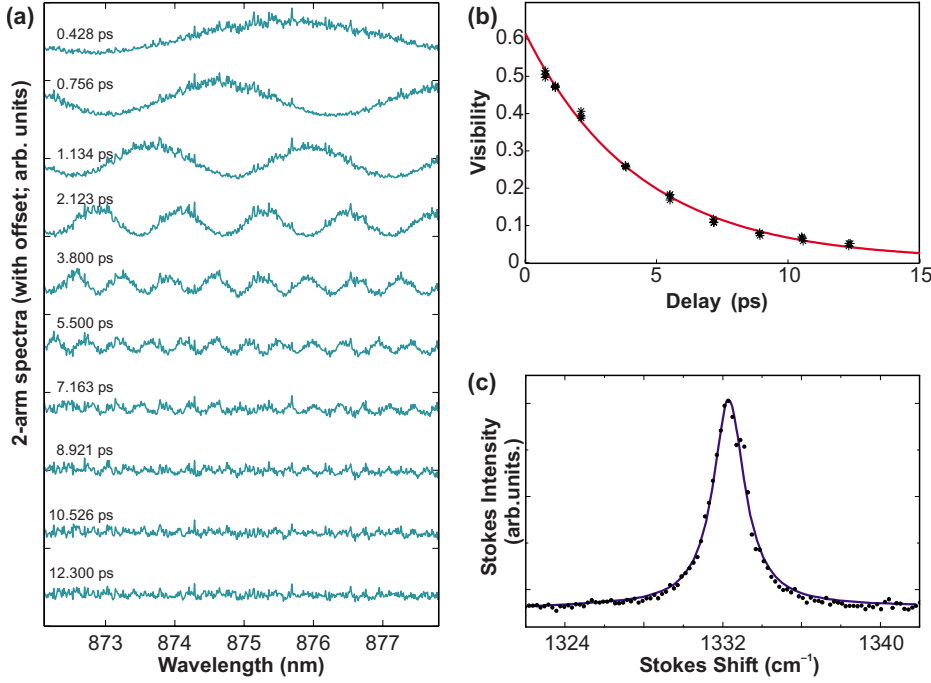


FIG. 4. (Color online) Decoherence measurement. (a) Stokes spectra for two pump pulses with various delays  $\tau$ , recorded with an 1800 lines/mm grating. The decrease in spectral interference visibility of the Stokes signal is due to decoherence of the optical phonons created. The respective visibilities are plotted in (b), obtained by curve-fitting the spectra. Asterisks denote data points, the continuous line an exponential decay fit. Part (c) shows a high-resolution Raman spectrum for the same diamond (dots) with a Lorentzian fit (line).

$$\langle |E_{\text{Stokes}}(\omega)|^2 \rangle_{\text{shots}} = 2|E_1(\omega)|^2 [1 + e^{-\Gamma|\tau|} \cos(\omega\tau)]. \quad (4)$$

The phase fluctuations cause a reduction of the fringe visibility.

Alternatively, the fluctuating phase perspective can be connected with the second quantum field perspective. This formalism can also be made applicable in the stimulated regime, although the process here is entirely in the spontaneous limit. The relationship between the stimulated and spontaneous cases is elaborated in the Appendix. The observed spectral intensity expectation value is proportional to the number of Stokes photons

$$\langle |E_{\text{Stokes}}(\omega)|^2 \rangle \propto \langle A^\dagger A \rangle, \quad (5)$$

where the lowering operator  $A(\omega)$  is a sum of the first  $A_1$  and second  $A_2$  pulse mode lowering operators

$$\langle |E_{\text{Stokes}}(\omega)|^2 \rangle \propto \langle A_1^\dagger A_1 \rangle + \langle A_2^\dagger A_2 \rangle + 2\Re \langle A_1^\dagger A_2 \rangle. \quad (6)$$

The final, correlated term [cf. the decay term in Eq. (4)] measures the phonon coherence that remains in the system between pulses. During the evolution of the system, the starting time phonon mode  $B^\dagger(0)$  is “mixed” into the Stokes photon modes  $A_i$  due to application of the laser field. The mixed-in term is then subsequently the source for spontaneous emission. The source term is the same for both pulses, but during the period between pulses the coherence is reduced due to crystal anharmonicity and impurities. That the source term is the same for both pulses indicates that the output Raman pulses will be phase coherent until overwhelmed by the fluctuations. For the correlation, the relevant terms to lowest perturbative order are (see Appendix for the equations of motion)

$$A_1 \approx A_1(0) - ig\tau_{\text{pump}} B^\dagger(0), \quad (7)$$

$$A_2 \approx A_1(0)e^{i\omega\tau} - ig\tau_{\text{pump}} B^\dagger(0)e^{-\Gamma\tau}, \quad (8)$$

from which the correlation term can be evaluated as

$$\langle A_1^\dagger A_2 \rangle \approx g^2 \tau_{\text{pump}}^2 \langle B(0) B^\dagger(0) \rangle e^{-\Gamma\tau} = g^2 \tau_{\text{pump}}^2 \langle N_B(0) + 1 \rangle e^{-\Gamma\tau}, \quad (9)$$

where  $N_B(0)$  is the initial number of phonons, which in this case is the nearly zero thermal population. This result links the phonon decoherence rate  $\Gamma$  with the fluctuating phase perspective linewidth  $\Gamma$  from Eq. (4). Therefore, measuring the reduction of the fringe visibility is a direct measure of the phonon dephasing time.

From the quantum field perspective, TCUPS is a type of two-slit experiment. For pulse durations much shorter than the decay time, the Hamiltonian during a pulse interaction is approximately of the form

$$H \approx gA^\dagger B^\dagger + g^* AB. \quad (10)$$

Therefore, the generated state from the first pulse (or slit) is equivalent to a two-mode squeezed vacuum state or a parametric down-conversion state.<sup>19</sup> As a result, the phonon mode and the photon mode are entangled. The fact that the phonon mode maintains its coherence for a time  $1/\Gamma$  permits the state prepared by the second pulse (or slit) to interfere with the first, creating a superposition. In the low intensity limit, only one Raman photon is created by a pump pulse pair. The inability to determine from which pump pulse the Raman photon was produced implies that there are two indistinguishable quantum paths ( $A_1$  and  $A_2$ ) which interfere at the detector to produce the observed fringes. However, as the time delay is increased, information about whether or not the Raman photon was created by the first pulse leaks into the surroundings via the phonon decoherence processes. This information can, in principle, be used to measure which-pulse

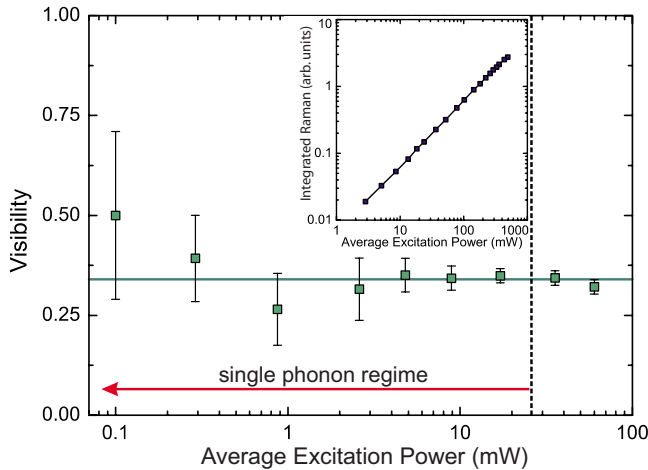


FIG. 5. (Color online) Power dependence. The power dependence of the Stokes interference visibility (at constant delay  $\tau=0.51$  ps, reduced due to a limited alignment) showing that the experiment can be carried out at arbitrarily low phonon excitation levels (the green horizontal line is plotted to guide the eyes). The inset shows the dependence of the Stokes pulse energy on the average pump power (single pump pulses). The linear power dependence shows that the scattering is in the spontaneous Raman regime. The fraction of pump power converted into collinear Stokes light was measured to be less than  $10^{-8}$ .

(which-path) information and therefore destroys the interference fringes.

#### IV. DISCUSSION

The TCUPS measurement indicates a phonon dephasing time of  $1/\Gamma=6.8\pm 0.9$  ps or a linewidth of  $\Delta\nu=1.56$   $\text{cm}^{-1}$ . The literature has reported a great deal of variation in linewidth measurements for diamond,<sup>6,18,20</sup> varying from at least  $1.1$   $\text{cm}^{-1}$  to as high as  $4.75$   $\text{cm}^{-1}$ . Here, the TCUPS [Fig. 4(b),  $\Delta\nu=1.56$   $\text{cm}^{-1}$ ] and conventional Raman spectrum [Fig. 4(c),  $\Delta\nu=1.95$   $\text{cm}^{-1}$ ] show comparatively good agreement. The lifetime measured here is slightly shorter than the decay rate calculated theoretically by Debernardi *et al.*<sup>21</sup> for an ideal crystal ( $\Delta\nu=1.01$   $\text{cm}^{-1}$  or  $1/\Gamma=10.5$  ps) as the decay process is enhanced by lattice imperfections, vacancies, and the high concentration of substitutional nitrogen atoms, as is typical for this sort of diamond. The decay model considering acoustic phonon modes suggests that this deviation from the theoretical optimum is due to inhomogeneous broadening rather than additional pure dephasing. Future work will reveal whether ultrapure diamond with very low crystal defect density can achieve a longer phonon lifetime. The creation of coherent phonons in diamond is heralded by the emitted Stokes photon, which could be employed for quantum optical experiments operating at room temperature, e.g., schemes that transfer optical entanglement to matter.<sup>22,23</sup>

The spectral interference pattern persists for low excitation levels, i.e., a phonon excitation probability per mode of  $p < 1$ . (The case of  $p \gg 1$  would correspond to a strongly stimulated regime, which has previously been studied in molecular hydrogen gas<sup>24</sup> although using spatial, not spectral,

interference.) A constant visibility with excitation power can be seen at low excitation level (Fig. 5). TCUPS can therefore be employed to measure the decoherence properties of single optical phonons, overcoming the need for large phonon populations for lifetime measurements of phonon decoherence.

The excitation probability per mode was much smaller than 1, ranging over  $p \approx 10^{-7} - 10^{-5}$  due to the large number of phonon modes in the Brillouin zone for which Stokes scatter is detected ( $\sim 10^5$ ). This level is in fact smaller than the thermal population level of the optical phonons at room temperature, given by  $p_{\text{thermal}} = [\exp(E_{\text{vib}}/k_B T) - 1]^{-1} \approx 0.0017$ . However, a small thermal population of the optical phonon modes does not influence this measurement method, as only the phonons deliberately excited by the pump pulses lead to Stokes scatter, and only Stokes light and its interference are detected. As phonons are governed by bosonic statistics, any finite background excitation level does not inhibit a further excitation. The linewidth increase due to phonon-phonon interaction is negligible at ambient temperatures in diamond due to the low population level.<sup>21</sup> An increase in the Raman linewidth of diamond due to temperature has been reported<sup>6</sup> to begin at around  $T \approx 300$  K. At  $T \approx 800$  K, it is more than twice the zero temperature linewidth. At room temperature, the phonon decay is only marginally enhanced by an acoustical phonon population. This insensitivity to a thermal background is in contrast to the differential reflectivity method, where thermal phonons lead to additional noise as both thermal and coherent phonons lead to a change in the material reflectivity.

With equipment found in a typical ultrafast laboratory, TCUPS is a convenient approach to determining the quantum coherence properties of optical phonons in Raman active solids. The measurement technique relies solely on spontaneous Raman scattering and is therefore useful down to the single phonon level. In particular, TCUPS enables the measurement of the decoherence time of phonons, which is of paramount importance in many quantum information processing schemes. Spectral interference of the Stokes light from pump pulse pairs is used to measure the Raman linewidth of the material, while maintaining a coherent excitation due to ultrafast excitation. The phonon lifetime of diamond was measured as 6.8 ps. This lifetime corresponds to a phonon  $Q$  factor of  $Q = \nu/\Gamma \sim 270$ . Although the short lifetime of the excitation makes it unsuitable for long-distance quantum repeaters, such a high  $Q$  and the low thermal population at room temperature make it feasible for proof-of-principle demonstrations of typical quantum optics schemes, such as collective-excitation entanglement in the solid state.

#### ACKNOWLEDGMENTS

This work was supported by the QIPIRC and EPSRC (Grant No. GR/S82176/01), EU RTN project EMALI, and Toshiba Research Europe.

#### APPENDIX: PHONON-PHOTON EQUATIONS OF MOTION

Consider an incident pump laser that Raman scatters off a phonon field of the diamond to produce an output Stokes



field. The equations of motion for Stokes field  $A(t)$  and the phonon field  $B(t)$  are linked by the pump coupling  $g$  via:<sup>25</sup>

$$\dot{A}(t) = -igB^\dagger(t) \quad (\text{A1})$$

and

$$\dot{B}(t) = -igA^\dagger(t) - \Gamma B(t) + F^\dagger(t). \quad (\text{A2})$$

The dephasing rate  $\Gamma$  is due to crystal anharmonicity and impurities. The Langevin operator  $F$  has been added to maintain the normalization of  $B$  in the presence of decay, allowing the phonon to decohere, but keeping the operator norm (via the commutation relation  $[B, B^\dagger]=1$ ) constant. The formal solutions are

$$B = B(0)e^{-\Gamma t} + \int_0^t e^{-\Gamma(t-t')} [-igA^\dagger(t') + F^\dagger(t')] dt' \quad (\text{A3})$$

and

$$A = A(0) - i \int_0^t gB^\dagger(t') dt'. \quad (\text{A4})$$

For brevity, the time argument has been dropped from the solutions. In the weak ( $g\tau_{\text{pump}} \ll 1$ ) and transient ( $\Gamma\tau_{\text{pump}} \ll 1$ ) pump pulse limits, the incident laser leaves the phonon operator approximately in the vacuum state  $B(0)$  and the phonon operator solution at lowest order is

$$B \approx B(0)e^{-\Gamma t} + \int_0^t e^{-\Gamma(t-t')} F^\dagger(t') dt'. \quad (\text{A5})$$

The Stokes field to first order is then

$$A \approx A(0) - ig\tau_{\text{pump}} B^\dagger(0)e^{-\Gamma t} - i \int_0^t \int_0^{t'} g e^{-\Gamma(t'-t'')} F(t'') dt'' dt', \quad (\text{A6})$$

where the coupling  $g$  in the second term has been taken as a constant step for the duration of the pump. The initial Stokes operator  $A(0)$  annihilates the vacuum, but the solution for  $A$  mixes in a component of the phonon raising operator  $B^\dagger(0)$ , which acts as a source for the spontaneous Raman scattering. While the source is in the weak spontaneous limit, the fact that a second pulse can scatter off the same mode  $B$  indicates

that the subsequent interference is phase coherent until destroyed by the fluctuation.

It is worthwhile to contrast the spontaneous case, discussed above, with that of the stimulated case. To do this we first rewrite the initial phonon state  $B(0)$  in terms of the fluctuations

$$B(0) = \int_{-\infty}^0 e^{-\Gamma t'} F^\dagger(t') dt', \quad (\text{A7})$$

noting that the initial state  $B(0)$  is due to the integrated fluctuations of the vacuum since the start of time. The initial system is devoid of phonon population such that  $\langle B^\dagger(0)B(0) \rangle = 0$ , however, as will be shown below, it is responsible for the coherence of spontaneous emission. Assuming constant coupling  $g$ , the approximate Eq. (A6) for the Stokes field, can be replaced with the exact equation

$$A = A(0) - ig \int_0^t \int_{-\infty}^{t'} e^{-\Gamma(t'-t'')} F(t'') dt'' dt' - g^2 \int_0^t \int_0^{t'} A(t'') e^{-\Gamma(t'-t'')} dt'' dt'. \quad (\text{A8})$$

The first term corresponds to initially present Stokes light, which is assumed to be zero here. The second term, which is first order in  $g$ , corresponds to spontaneous emission. In the presence of weak coupling this is the only source of Stokes to first order and occurs even in the absence of any phonon population. The third and final term corresponds to stimulated emission. While the phonon operator  $B$  is not explicit in the third term, it is implicitly present through its coupling to  $A(t'')$ . TCUPS utilizes emission only from the second term despite the absence of any phonon population. The spontaneous Raman emission from two time-delayed pulses is correlated provided the initial vacuum fluctuations have not appreciably dephased. This is in contrast to interference between stimulated emissions. In the stimulated limit, the phonon state is populated and the emission of a pulse pair is coherent because the phase of the phonon population created by the first pulse is mapped onto that created by the second.

The decoherence rate  $\Gamma$  represents the dephasing of the phonon raising operator  $B^\dagger$ . The phonon number  $N_B = B^\dagger B$  therefore decays at a rate  $2\Gamma$ . The corresponding spectral frequency linewidth is  $\Delta\nu = \Gamma/\pi$ .

\*Also at National Research Council of Canada, Ottawa, Ontario, Canada K1A 0R6; ben.sussman@nrc.ca

<sup>1</sup>*Properties of natural and synthetic diamond*, edited by J. E. Field (Academic Press, London, 1992).

<sup>2</sup>Jörg Wrachtrup and Fedor Jelezko, *J. Phys.: Condens. Matter* **18**, S807 (2006).

<sup>3</sup>L. Childress, M. V. Gurudev Dutt, J. M. Taylor, A. S. Zibrov, F. Jelezko, J. Wrachtrup, P. R. Hemmer, and M. D. Lukin, *Science* **314**, 281 (2006).

<sup>4</sup>P. Neumann, N. Mizuochi, F. Rempp, P. Hemmer, H. Watanabe,

S. Yamasaki, V. Jacques, T. Gaebel, F. Jelezko, and J. Wrachtrup, *Science* **320**, 1326 (2008).

<sup>5</sup>F. C. Waldermann, P. Olivero, J. Nunn, K. Surmacz, Z. Y. Wang, D. Jaksch, R. A. Taylor, I. A. Walmsley, M. Draganski, P. Reichart, A. D. Greentree, D. N. Jamieson, and S. Praver, *Diamond Relat. Mater.* **16**, 1887 (2007).

<sup>6</sup>M. S. Liu, L. A. Bursill, S. Praver, and R. Beserman, *Phys. Rev. B* **61**, 3391 (2000).

<sup>7</sup>G. C. Cho, W. Kütt, and H. Kurz, *Phys. Rev. Lett.* **65**, 764 (1990).

- <sup>8</sup>T. K. Cheng, S. D. Brorson, A. S. Kazeroonian, J. S. Moodera, G. Dresselhaus, M. S. Dresselhaus, and E. P. Ippen, *Appl. Phys. Lett.* **57**, 1004 (1990).
- <sup>9</sup>Yong-Sik Lim, Seok-Chan Yoon, Ki-Ju Yee, Jai-Hyung Lee, D. S. Kim, and Donghan Lee, *Phys. Rev. B* **68**, 153308 (2003).
- <sup>10</sup>Muneaki Hase, Masahiro Kitajima, Anca Monia Constantinescu, and Hrvoje Petek, *Nature (London)* **426**, 51 (2003).
- <sup>11</sup>A. Bartels, T. Dekorsy, and H. Kurz, *Phys. Rev. Lett.* **84**, 2981 (2000).
- <sup>12</sup>S. De Silvestri, J. G. Fujimoto, E. P. Ippen, Edward B. Gamble, Leah Ruby Williams, and Keith A. Nelson, *Chem. Phys. Lett.* **116**, 146 (1985).
- <sup>13</sup>Y. Liu, A. Frenkel, G. A. Garrett, J. F. Whitaker, S. Fahy, C. Uher, and R. Merlin, *Phys. Rev. Lett.* **75**, 334 (1995).
- <sup>14</sup>N. Bloembergen, M. J. Colles, J. Reintjes, and C. S. Wang, *Indian J. Pure Appl. Phys.* **9**, 874 (1971).
- <sup>15</sup>K. Ishioka, M. Hase, M. Kitajima, and H. Petek, *Appl. Phys. Lett.* **89**, 231916 (2007).
- <sup>16</sup>K. J. Yee, K. G. Lee, E. Oh, D. S. Kim, and Y. S. Lim, *Phys. Rev. Lett.* **88**, 105501 (2002).
- <sup>17</sup>Alexander M. Zaitsev, *Optical Properties of Diamond* (Springer, New York, 2001).
- <sup>18</sup>A. Laubereau, D. von der Linde, and W. Kaiser, *Phys. Rev. Lett.* **27**, 802 (1971).
- <sup>19</sup>Marlan O. Scully and M. Suhail Zubairy, *Quantum Optics* (Cambridge University Press, Cambridge, England, 1997).
- <sup>20</sup>Kuei-Hsien Chen, Yen-Liang Lai, Li-Chyong Chen, Jin-Yu Wu, and Fu-Jen Kao, *Thin Solid Films* **270**, 143 (1995).
- <sup>21</sup>A. Debernardi, S. Baroni, and E. Molinari, *Phys. Rev. Lett.* **75**, 1819 (1995).
- <sup>22</sup>D. N. Matsukevich and A. Kuzmich, *Science* **306**, 663 (2004).
- <sup>23</sup>C. W. Chou, H. de Riedmatten, D. Felinto, S. V. Polyakov, S. J. van Enk, and H. J. Kimble, *Nature (London)* **438**, 828 (2005).
- <sup>24</sup>M. Belsley, D. T. Smithey, K. Wedding, and M. G. Raymer, *Phys. Rev. A* **48**, 1514 (1993).
- <sup>25</sup>M. G. Raymer and I. A. Walmsley, *Prog. Opt.* **23**, 181270 (1990).